Determining the Optimum Layer Combination for Cross-Laminated Timber Panels According to Timber Strength Classes Using Artificial Neural Networks

Engin Derya Gezer,[a,*] Abdullah Uğur Birinci,[a] Aydın Demir,[a] Hasan Öztürk,[b,c] Okan İlhan,[a] and Cenk Demirkir [a,c]

*Corresponding author: gezer@ktu.edu.tr

DOI: 10.15376/biores.19.3.4899-4917

GRAPHICAL ABSTRACT

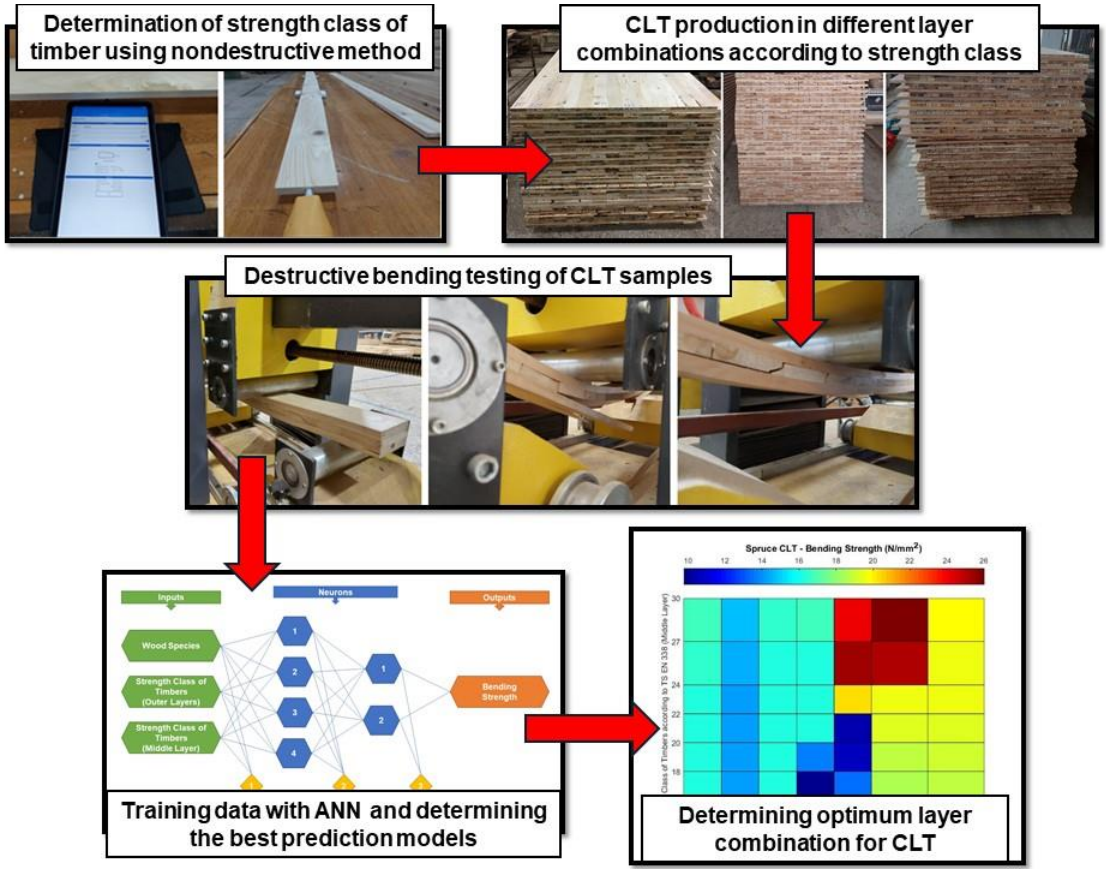

Determining the Optimum Layer Combination for Cross-Laminated Timber Panels According to Timber Strength Classes Using Artificial Neural Networks

Engin Derya Gezer,[a,*] Abdullah Uğur Birinci,[a] Aydın Demir,[a] Hasan Öztürk,[b,c] Okan İlhan,[a] and Cenk Demirkir [a,c]

The primary aim of this work was to determine the effects of production parameters, such as wood species and timber strength classes, on some mechanical properties of cross-laminated timber (CLT) panels using artificial neural network (ANN) prediction models. Subsequently, using the models obtained from the analyses, the goal was to identify the optimum layer combinations of timber strength classes used in the middle and outer layers that would provide the highest mechanical properties for CLT panels. CLT panels made from spruce and alder timbers, as well as hybrid panels created from combinations of these two wood species, were produced. The strength classes of the timbers were determined non-destructively according to the TS EN 338 (2016) standard using an acoustic testing device. The bending strength and modulus of elasticity values of the CLT panels were determined destructively according to the TS EN 408 (2019) standard. According to ANN results, the optimum timber strength classes and layer combinations were determined for bending strength as C24-C27-C24 for spruce CLT, D18-D24-D18 for alder CLT, C30-D40-C30 and D18-C30-D18 for hybrid panels; and for modulus of elasticity, C22-C27-C22 for spruce, D35-D30-D35 for alder, C16-D24-C16, and D24-C24-D24 for hybrid panels.

DOI: 10.15376/biores.19.3.4899-4917

Keywords: Artificial neural network (ANN); Cross-laminated timber (CLT); Strength class; Non-destructive testing

*Contact information: a: Karadeniz Technical University, Faculty of Forestry, Department of Forest Industry Engineering, 61080, Trabzon, Türkiye; b: Karadeniz Technical University, Arsin Vocational School, Department of Materials and Material Processing Technologies, 61900, Trabzon, Türkiye; c: Trabzon Technology Development Region Manager, HC Panel Forest Products Consulting Services Industry and Trade Limited Company, 61081, Trabzon, Türkiye; *Corresponding author: gezer@ktu.edu.tr*

INTRODUCTION

Wood is recognized for its carbon storing ability, renewability, reusability, recyclability, lower carbon impact, it is environmentally benign, and promotes good health (Di Bella and Mitrovic 2020). Wood construction technologies are widely employed throughout many regions globally. Out of all the options, cross-laminated timber (CLT) stands out as the most captivating and groundbreaking material for wooden construction. CLT is considered a desirable material for various types of buildings, including detached houses, multi-story buildings, schools, auditoriums, exhibition centers, sports halls, theaters, commercial establishments, and religious buildings. This is due to its advantageous characteristics, such as its lighter weight compared to concrete and steel, its

quick construction time, its low carbon footprint, and its ability to withstand earthquakes (Di Bella and Mitrovic 2020; Hindman and Golden 2020; Hematabadi *et al*. 2020).

At present, the primary raw material for producing CLT panels on a commercial scale is derived from three main coniferous wood species: spruce, pine, and fir (Srivaro *et al.* 2020). Recent studies have explored the use of fast-growing tree species to broaden the raw material source and enhance the qualities of CLT or hybrid CLT (Dong *et al.* 2023). Studies have identified poplar, eucalyptus, magnolia, and bamboo as often utilized fast-growing tree or non-wood species in the manufacture of CLT (Marko *et al.* 2016; Liao *et al.* 2017; Dong *et al.* 2023; Satir 2023; Shi *et al.* 2023). There is a lack of research in the existing literature regarding the utilization of alder timbers, a rapidly growing tree species indigenous to Turkey, in the manufacturing of CLT. This study successfully manufactured CLT panels utilizing alder and spruce timbers, as well as hybrid panels combining these two wood species.

The selection of wood species for the manufacture of structural material is crucial, with the quality and strength class of the chosen species being key criteria that significantly impact the quality of CLT. The TS EN 338 (2016) European standard has established a strength classification for coniferous wood species, consisting of 12 groups (C14, C16, C18, C20, C22, C24, C27, C30, C35, C40, C45, and C50). Similarly, deciduous wood species have been categorized into 8 groups (D18, D24, D30, D35, D40, D50, D60, and D70). These classifications not only ascertain the caliber of the timber but also have a substantial impact on its selling price. According to literature research, European big enterprises that produce CLT typically utilize timbers classified as C24 strength classes based on the TS EN 338 (2016) standard (Wieruszewski and Mazela 2017). Furthermore, companies such as Binderholz, from Austria, utilize a minimum of C18 strength values. In addition, Stora Enso employs C16 and C30 values, Thoma Holz GmbH uses C16 values, Martinsons from Sweden uses at least C14 values, and Lignotrend AG from Switzerland can incorporate both C20 and C24 strength values (Wieruszewski and Mazela 2017). Previous studies in the literature have noted that coniferous wood species are commonly utilized in the production of CLT. However, these studies have primarily focused on a single group, typically C24, instead of comparing strength values. Among the notable studies on this subject are those by Hassanieh *et al*. (2017), Reynolds *et al*. (2017), Follesa and Fragiancomo (2018), Brandner (2018), Turesson *et al*. (2019), and Lie *et al*. (2020). In addition, strength classes, such as C16 (Kippel *et al.* 2014), C18 (Soriano *et al.* 2016; Luengo *et al.* 2017), C22 (Guo *et al.* 2017), and C30 (Hadigheh and Dias da Costa 2020), have also been favored. O'Dowd *et al.* (2016) reported the utilization of timbers from two distinct strength classes in the manufacturing of a single CLT panel. This study specifically chose three distinct strength classes of spruce and alder timbers and utilized various layer combinations to create CLT. It is worth noting that a full investigation into strength classes of this nature has not been documented in the existing literature.

Cost and time-effective testing can be conducted to determine the technological qualities of CLT materials. Nevertheless, altering the production parameters of CLT could result in a procedure that may incur expenses and delays when establishing the potential strength values, considering various elements. Currently, it is feasible to forecast the strength characteristics of wood material under various manufacturing settings by utilizing an Artificial Neural Network (ANN) approach to model the data acquired from existing testing. According to literature research, ANNs have been effective in optimizing structural timber materials. Demir *et al.* (2023) investigated the impact of certain production parameters on the structural behavior of plywood-sheathed walls when subjected to lateral

load. They successfully obtained optimal outcomes by utilizing the ANN to model the nail spacing during production. Öztürk *et al.* (2022) investigated how press parameters impacted the mechanical properties of composite plywood. They utilized ANN models to determine the optimal press settings that yield the maximum strength values. In addition, Demirkir *et al.* (2013) utilized ANN models to identify the optimal values for certain production factors that yielded the greatest adhesive strength in plywood. The objective of this study was to assess the impact of production characteristics, specifically wood species, and wood strength class, on the mechanical properties of CLT panels using ANN. In addition, the objective was to identify the optimal combinations of timber strength classes in the intermediate and outer layers of CLT panels that would yield the maximum mechanical properties. This was achieved through optimization studies utilizing ANN models.

EXPERIMENTAL

Wood Material

In this study, spruce (*Picea orientalis* L.), a coniferous wood species, was selected as one of the most preferred types for CLT production. Additionally, alder (*Alnus glutinosa* subsp. *barbata* (C.A. Mey.) Yalt.), a type of deciduous tree known for its rapid growth, was chosen. Timber from both species was sourced from different regions, in three different quality classes for spruce and two different quality classes for alder, according to the appearance characteristics specified in the TS 1265 (2012) and TS EN 14081-1 (2019) standards, respectively. The timber was planed on all four sides and supplied dry. Care was taken to ensure that the timber had a moisture content within the most suitable range for CLT production, which is 12 ± 3%. Before CLT production, the timbers were dimensioned to sizes of 120 × 10 × 1.8 cm^3 and 240 × 10 × 1.8 cm^3.

Determination of Timber Strength Classes

The parameters used in this study made it possible to find out the strength classes of the woods before they were used to make CLT. This was done by using non-destructive testing methods that followed the TS EN 338 (2016) Standard. The timbers were obtained based on their visual qualities. The Sylvatest 4 acoustic testing instrument, developed by CBS-CBT, was utilized to ascertain the strength classes of the timber (Fig. 1).

Fig. 1. Determining the strength classes of timber with an acoustic testing device

The instrument uses software to determine the bending strength and modulus of elasticity directly from the measurement of the ultrasonic wave flight duration in the wood material between two transducers (the transmitter and receiver). It then displays the strength class in accordance with the applicable standard. It also creates a graph from the acquired data (Fig. 2). Because the alder wood species is not included among the tree species in the device's software, the MOE values for this wood species were calculated using the Eq. 1 given below,

$$MOE = V^2 x\, d \quad (1)$$

where V is the velocity obtained from the device and d is the density of the alder lumber pieces.

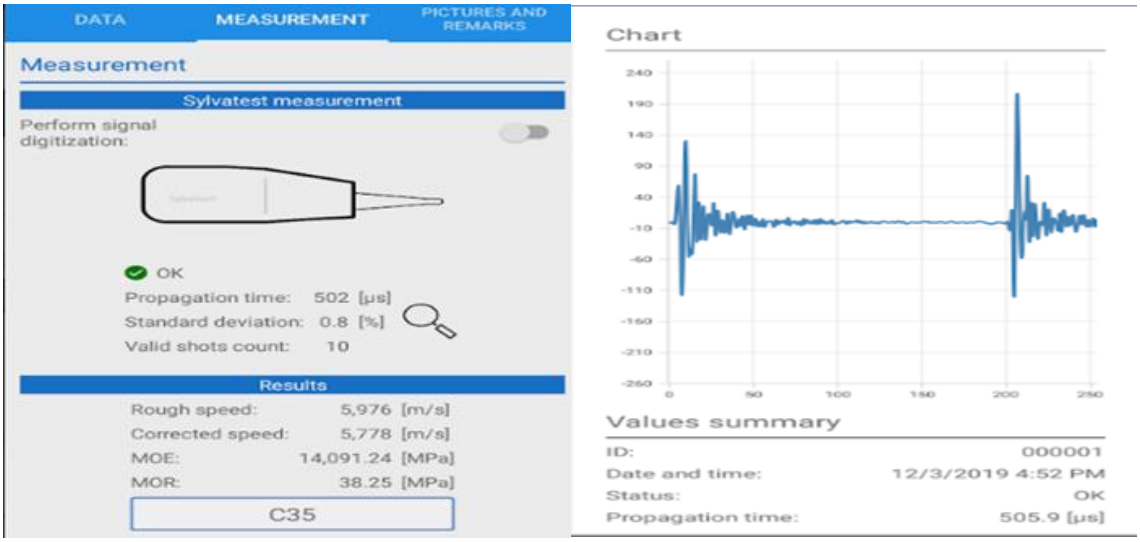

Fig. 2. Acoustic testing device software data

A non-destructive test was performed on 1876 spruce and 1063 alder lumber pieces obtained according to visual quality class. The non-destructive tests yielded strength classes C and D, respectively, for spruce and alder timbers, in accordance with the TS EN 338 (2016) standard. Within the parameters of this investigation, timbers of spruce (C16, C22, and C30) and alder (D18, D30, and D40) were chosen for use in CLT manufacturing based on the obtained strength class groups. The distribution graphs of the MOR and MOE for spruce and alder lumbers are shown in Fig. 3.

Production of CLT Panels

A 160 g/cm^2 polyurethane adhesive solution was put on the wood's surfaces in the layer combination groups. These groups were made using the types of wood and strength classes listed in the TS EN 338 (2016) standard. The design process for the manufactured CLT panels involved arranging the layers perpendicularly. In the process of drafting, the orientation of the annual rings in the cross-sections of the timbers was considered to reduce the material shrinkage and swelling. This resulted in the creation of drafts using alder, spruce, and hybrid (alder and spruce combination) timbers. The draft boards were prepared to have three layers and then underwent a pressing procedure. The hydraulic press used for the draft pressing was capable of exerting both vertical and lateral pressures, meeting the requirements of industrial settings.

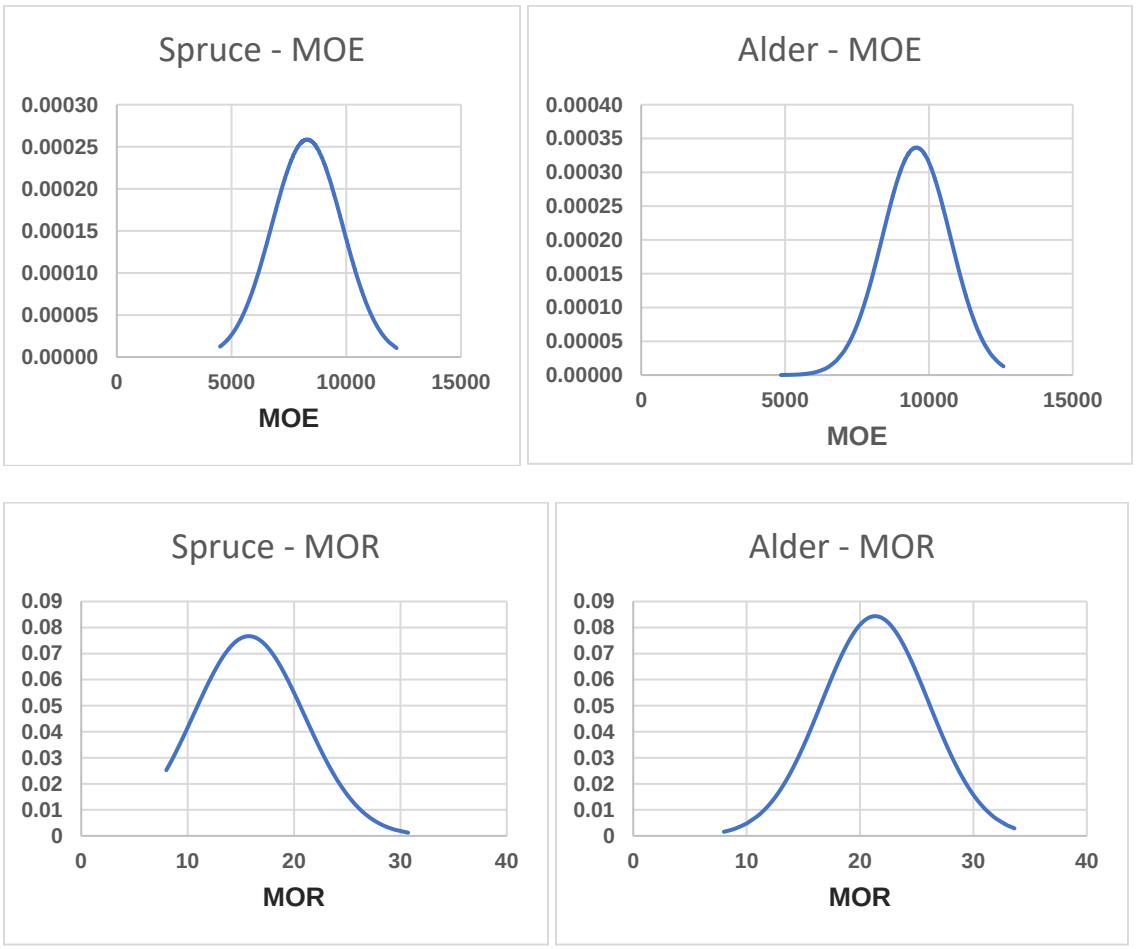

Fig. 3. The distribution of the MOR and MOE for spruce and alder lumbers

The pressing method involved the use of a cold press. The applied pressure was 0.8 N/mm^2 for spruce and hybrid, and 1.2 N/mm^2 for alder. To reduce the space between the wood pieces, a lateral pressing technique was employed, applying pressure ranging from 0.276 to 0.550 N/mm^2 in conjunction with vertical pressing (Karacabeyli and Gagnon 2019). Table 1 presents the 30 test groups that were generated by combining different wood species with the TS EN 338 (2016) standard.

Destructive Testing of CLT Panels

The bending strength and modulus of elasticity tests for the CLT panels were conducted according to the TS EN 408 (2014) standard, which is used to determine the mechanical and physical properties of structural timber and glued laminated timber. For the bending strength and modulus of elasticity tests, six samples (replicates) from each group were taken.

ANN Modeling

Three distinct strength categories were established for spruce and alder timbers utilized in the manufacturing of CLT panels. During the evaluation, consideration was made based on the TS EN 338 (2016) standard that coniferous timber with strength classes C45 and C50 may not be accessible.

Table 1. Test Groups Formed According to Wood Species and TS EN 338 (2016) Standard

Group Number	Wood Species	Layer Combinations
1	Spruce	C16 - C16 - C16
2		C22 - C22 - C22
3		C30 - C30 - C30
4		C16 - C22 - C16
5		C22 - C16 - C22
6		C16 - C30 - C16
7		C30 - C16 - C30
8		C22 - C30 - C22
9		C30 - C22 - C30
10	Alder	D18 - D18 - D18
11		D30 - D30 - D30
12		D40 - D40 - D40
13		D18 - D30 - D18
14		D30 - D18 - D30
15		D18 - D40 - D18
16		D40 - D18 - D40
17		D30 - D40 - D30
18		D40 - D30 - D40
19	Hybrid	C16 - D18 - C16
20		C22 - D30 - C22
21		C30 - D40 - C30
22		D18 - C16 - D18
23		D30 - C22 - D30
24		D40 - C30 - D40
25		C16 - D30 - C16
26		C16 - D40 - C16
27		C22 - D40 - C22
28		D18 - C22 - D18
29		D18 - C30 - D18
30		D30 - C30 - D30

Additionally, no research studies were found regarding the utilization of timber with strength classes higher than C30 in the production of CLT. Thus, the groups were chosen based on the strength class selection, which included C16, C22, and C30 for coniferous and D18, D30, and D40 for deciduous wood species.

The selection was made to ensure equal spacing between the classification rankings specified in the applicable standard, up to the C30 standard. The objective of the ANN modeling in this study was to determine the strength values for different strength classes according to the TS EN 338 (2016) standard using experimental data gathered from three strength classes. Therefore, the study was able to accurately predict the structural strength of CLT panels that would be made from timbers with different strength classes. This meant that expensive and time-consuming tests were not needed, and the results were very reliable. ANN studies were also used to make prediction models that helped find the best combinations of wood strength classes for spruce, alder, and hybrid CLT panels for both the outer and middle layers.

The main process variables (inputs) used in this ANN modeling were the wood species and the strength class values of the timbers used in the outer and inner layers, according to TS EN 338 (2016). The output variables consisted of the bending strength and

modulus of elasticity values, which represented the mechanical strength properties of the CLT panels. The MATLAB software package was utilized for the creation, training, and testing of artificial neural networks, ultimately leading to the identification of optimal values. The results were acquired *via* experimental research conducted in a manner that caused damage or destruction. To find out how the strength properties changed when different wood species and strength classes of wood were used in the outer and middle layers, as described in TS EN 338 (2016), the experimental data was split into training and test sets. Out of the available data, 20 examples were chosen for the training phase of the ANN, while the remaining 10 samples were utilized to assess the ANN's ability to validate prediction capability. The estimated values obtained from the test process were compared to the actual values. The prediction models that yielded the most accurate predictions were selected based on the root mean square error (RMSE) calculated using Eq. 2 and the mean absolute percentage error (MAPE) calculated using Eq. 2. These diagnostic measures are widely recognized as the best and most commonly used indicators of performance. These equations are as follows,

$$\text{RMSE} = \sqrt{\frac{1}{N}\sum_{i=1}^{N}(t_i - td_i)^2} \quad (2)$$

$$\text{MAPE} = \frac{1}{N}\left(\sum_{i=1}^{N}\left[\left|\frac{t_i - td_i}{t_i}\right|\right]\right) \times 100 \quad (3)$$

where t_i represents the actual value, td_i represents the model prediction value, and N refers to the number of terms. The network architectures identified as the top-performing prediction models in ANN analyses are shown in Figs. 4 and 5, based on the output variables. The network topologies of the models that yield the most accurate and precise results are shown in the pictures. These structures comprise of 1 input layer, 2 hidden layers, and 1 output layer. Each hidden layer consisted of 4 to 2 neurons for measuring bending strength and 3 to 5 neurons for measuring modulus of elasticity, respectively.

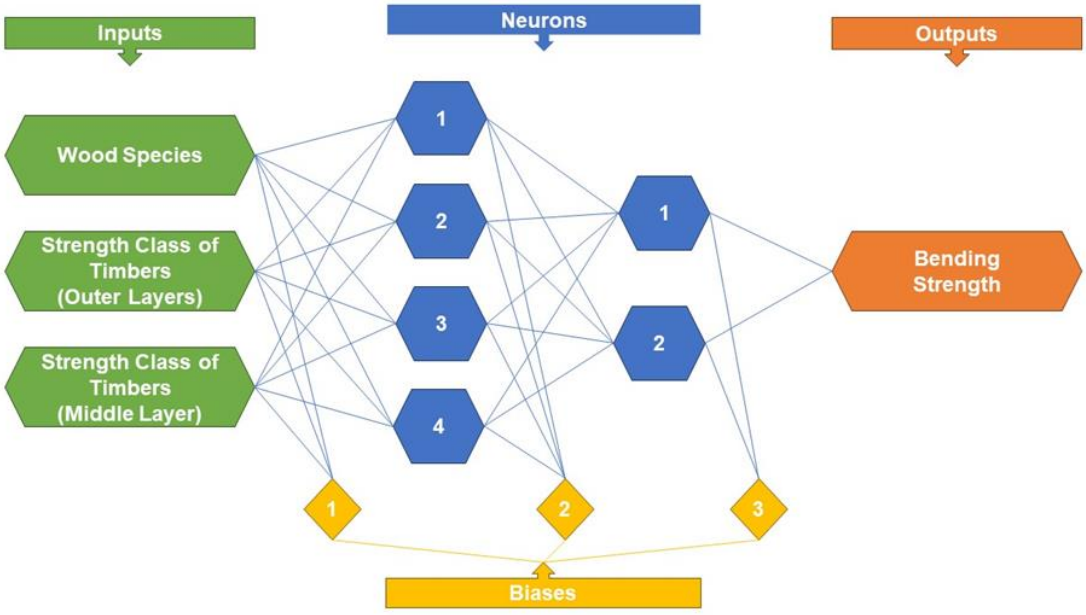

Fig. 4. The ANN architecture selected as the bending strength prediction model

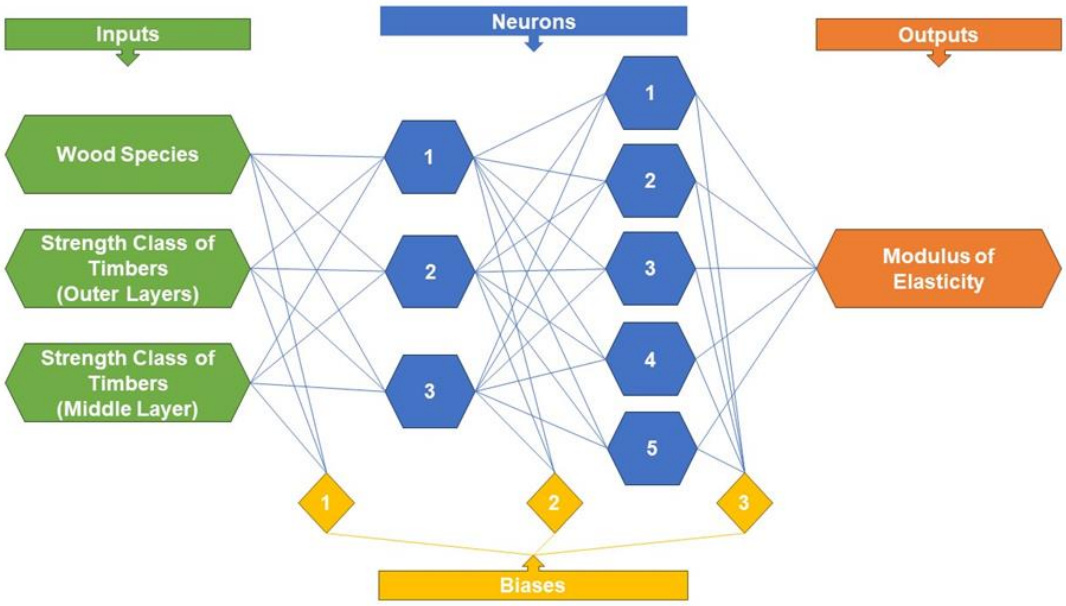

Fig. 5. The ANN architecture selected as the elasticity modulus prediction model

A multilayer feedforward and backpropagation ANN has been chosen as the preferred method for handling the challenges. The activation functions chosen for this investigation are the hyperbolic tangent sigmoid function (tansig) and the linear transfer function (purelin). The learning rule chosen for the neural network was the gradient descent with momentum backpropagation algorithm (traingdm), while the training technique picked was the Levenberg-Marquardt algorithm (trainlm). The performance function utilized for evaluation was the mean square error (MSE), which was computed using Eq. 4:

$$\text{MSE} = \frac{1}{N}\sum_{i=1}^{N}(t_i - td_i)^2 \quad (4)$$

The training and test data were standardized to the range of (-1,1) in the models constructed using the hyperbolic tangent sigmoid function. This normalization ensured that each variable had an equal impact on the prediction models. Afterwards, to guarantee an accurate understanding of the outcomes, the data underwent a reverse normalizing procedure to revert them to their initial values. The normalization (scaling) procedures were computed using Eq. 4. The equation defines the variables as follows: X_{norm} represents the data that has been normalized, X represents the actual value of the variable, X_{min} represents the minimum value in the data set, and X_{max} represents the highest value in the data set.

RESULTS AND DISCUSSION

ANN Modeling

The study successfully obtained extremely dependable and accurate prediction models using destructive structural strength values. During the analysis, a multitude of models were trained and tested. The models that yielded the most accurate predictions were

determined based on the MSE values. Figure 6 depicts the variations in these values over the course of the iterations.

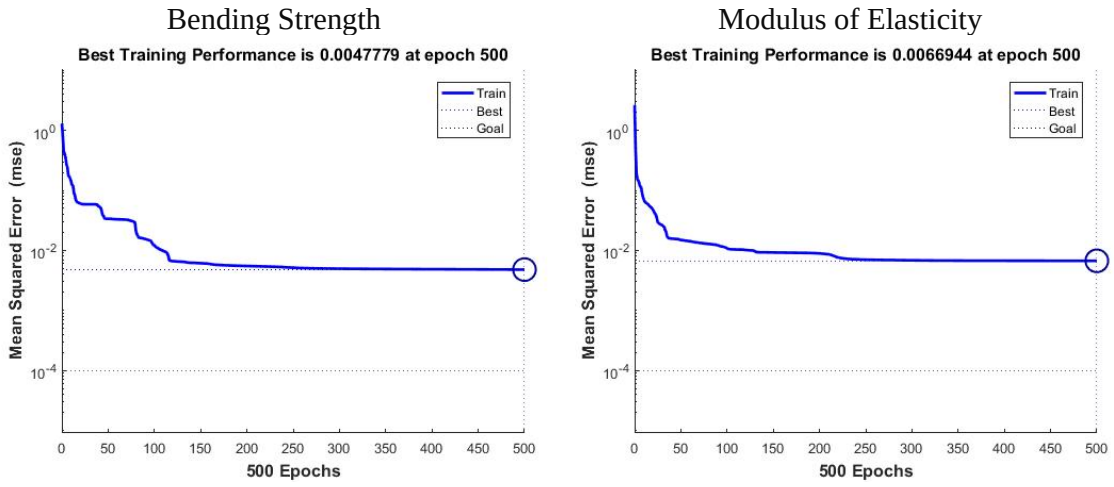

Fig. 6. MSE changes of the determined prediction models depending on the iteration

Figure 6 clearly shows that the prediction models achieved their highest results for bending strength and modulus of elasticity values at the 500th iteration, with values of 0.0047779 and 0.0066944, respectively. Table 2 displays the experimental results of the training and test datasets utilized in the prediction models, which exhibited high-performance values. The table also presents the prediction results and corresponding error rates. Additionally, the MAPE and RMSE values computed for the models are shown in Table 2.

Table 2 shows that the experimental and prediction data for CLT panels achieved a strong correlation with low error rates. The maximum error rates for bending strength data were determined as 7.47% for spruce, 8.48% for alder and 8.51% for hybrid CLT panels. The results showed that the highest error rates for modulus of elasticity data were 4.93% for hybrid. 8.60% for spruce and 8.52% for alder CLT panels.

The MAPE and RMSE values associated with the prediction models presented in the table further demonstrate the extent of this agreement. Specifically, MAPE is a crucial evaluation criterion and numerous studies have evaluated model performance using MAPE (Antanasijević *et al.* 2013; Yadav and Nath 2017). According to Yadav and Nath (2017), a model's performance is regarded as high if the MAPE value is less than 10%. The study established the MAPE values for bending strength as 1.04% for the training data and 3.90% for the test data. Similarly, for the modulus of elasticity, the MAPE values were computed as 1.95% for the training data and 4.26% for the test data. The error levels indicated that the ANN prediction models yielded satisfactory and effective outcomes, demonstrating sufficient accuracy and reliability.

When selecting the optimal ANN model, both RMSE values and MAPE values should be considered (Küçükönder *et al.* 2016). A low RMSE value is a parameter that indicates the strong performance of a model (Taşpınar and Bozkurt 2014). The RMSE values for bending strength training and test data were estimated as 0.37 and 0.74. respectively, for modulus of elasticity, these values were determined as 334 and 585, respectively. These error levels demonstrated their adequacy for the prediction models of

bending strength and modulus of elasticity values. Tables 3 and 4 provide the connection weights and bias values for the prediction models.

Table 2. Training and Test Data on Bending Strength and Modulus of Elasticity Values

Training Data							
Wood Species	Layer Combinations	Bending Strength (N/mm²)			Modulus of Elasticity (N/mm²)		
		Actual	Predicted	Error (%)	Actual	Predicted	Error (%)
Spruce	C22 - C22 - C22	20.35	20.35	0.01	12405.00	12614.38	-1.69
Spruce	C30 - C30 - C30	19.60	19.60	-0.02	13291.38	13254.22	0.28
Spruce	C22 - C16 - C22	13.55	13.56	-0.05	10667.49	10737.61	-0.66
Spruce	C16 - C30 - C16	16.69	16.69	-0.01	8904.05	8946.12	-0.47
Spruce	C30 - C16 - C30	18.73	18.70	0.14	12805.93	12935.29	-1.01
Spruce	C30 - C22 - C30	19.24	19.26	-0.10	13087.41	12738.68	2.66
Alder	D18 - D18 - D18	10.18	10.18	0.00	9846.02	9845.94	0.00
Alder	D40 - D40 - D40	16.45	16.45	0.00	13340.39	12859.24	3.61
Alder	D18 - D30 - D18	14.89	14.89	0.01	10651.16	9735.28	8.60
Alder	D30 - D18 - D30	9.79	9.76	0.31	6712.05	6744.93	-0.49
Alder	D30 - D40 - D30	12.00	12.00	0.00	9091.04	9867.87	-8.55
Alder	D40 - D30 - D40	9.77	9.76	0.11	10138.68	10000.39	1.36
Hybrid	C16 - D18 - C16	11.77	11.91	-1.17	11312.98	11309.58	0.03
Hybrid	C22 - D30 - C22	15.47	14.29	7.61	12998.63	13144.50	-1.12
Hybrid	D18 - C16 - D18	11.44	11.27	1.53	9461.30	9403.35	0.61
Hybrid	D40 - C30 - D40	10.88	10.88	0.00	10221.66	10345.54	-1.21
Hybrid	C16 - D30 - C16	10.77	10.77	0.00	11539.11	11539.38	0.00
Hybrid	C22 - D40 - C22	10.03	10.11	-0.77	11351.45	11880.85	-4.66
Hybrid	D18 - C22 - D18	13.24	14.35	-8.37	9097.35	9158.31	-0.67
Hybrid	D30 - C30 - D30	12.51	12.58	-0.52	10307.80	10174.38	1.29
MAPE		**1.04**			**1.95**		
RMSE		**0.37**			**333.62**		
Testing Data							
Wood Species	Layer Combinations	Bending Strength (N/mm²)			Modulus of Elasticity (N/mm²)		
		Actual	Predicted	Error (%)	Actual	Predicted	Error (%)
Spruce	C16 - C16 - C16	16.96	16.19	4.57	10109.14	10187.12	-0.77
Spruce	C16 - C22 - C16	13.77	14.21	-3.16	11094.82	10946.03	1.34
Spruce	C22 - C30 - C22	17.19	18.47	-7.47	11757.49	10755.48	8.52
Alder	D30 - D30 - D30	11.56	11.76	-1.73	12252.38	13186.77	-7.63
Alder	D18 - D40 - D18	14.92	16.19	-8.48	10236.47	9405.92	8.11
Alder	D40 - D18 - D40	11.90	11.76	1.18	10531.10	10570.54	-0.37
Hybrid	C30 - D40 - C30	16.65	16.42	1.38	14867.10	15463.17	-4.01
Hybrid	C16 - D40 - C16	12.98	11.87	8.51	10661.48	10136.07	4.93
Hybrid	D30 - C22 - D30	9.83	9.76	0.72	8983.15	8611.02	4.14
Hybrid	D18 - C30 - D18	14.25	14.51	-1.83	8606.04	8843.59	-2.76
MAPE		**3.90**			**4.26**		
RMSE		**0.74**			**585.06**		

Table 3. Connection Weights and Biases of the Prediction Model of Bending Strength Values

Hidden Layer 1	**Neuron 1**	**Neuron 2**	**Neuron 3**	**Neuron 4**	**Bias 1**
	1.26	1.41	-12.43	-4.60	-9.16
	10.13	-3.39	-0.96	-4.26	1.25
	-0.75	3.19	0.08	2.82	-5.90
	-	-	-	-	-5.38
Hidden Layer 2	**Neuron 1**	**Neuron 2**	**Bias k2**		
	24.10	-1.10	-17.22		
	40.59	1.65	-1.03		
	41.17	3.60	-		
	-41.88	9.28	-		
Output Layer	**Neuron 1**	**Bias 3**	**-**		
	0.93	0.54	-		
	0.61	-	-		

Table 4. Connection Weights and Biases of the Prediction Model of Modulus of Elasticity Values

Hidden Layer 1	**Neuron 1**	**Neuron 2**	**Neuron 3**	**Bias 1**		
	-9.50	-2.56	4.53	-10.80		
	-0.15	-1.27	-4.90	0.18		
	1.49	1.34	-3.96	-6.66		
Hidden Layer 2	**Neuron 1**	**Neuron 2**	**Neuron 3**	**Neuron 4**	**Neuron 5**	**Bias 2**
	-1.22	-1.12	-3.28	-6.67	-0.94	3.09
	-1.04	-1.02	0.74	1.57	0.34	1.72
	-1.58	-2.31	0.36	0.40	3.08	-3.16
	-	-	-	-	-	-6.42
	-	-	-	-	-	-1.62
Output Layer	**Neuron 1**	**Bias 3**				
	-0.64	0.89				
	0.06	-				
	-13.03	-				
	8.56	-				
	2.20	-				

Regression analyses are crucial for evaluating the validity and accuracy of prediction models. They involve calculating the relationship between data from experimental studies and prediction data obtained from analyses. The predictive accuracy of the models improves as the correlation coefficients (R) approach 1.0 (Özşahin 2012). Figure 7 presents the R and regression graphs for the prediction models based on the output variable as a result of the analysis.

When Fig. 6 is examined, the R-values for the training and testing phases of the bending strength prediction model were determined as 0.99446 and 0.96191, respectively. The modulus of the elasticity prediction model yielded an R-value of 0.98135 during the training phase and 0.96213 during the testing phase. Based on the R values, the high correlation coefficients near 1.0 provide statistical evidence that there is a strong agreement between the experimental data and the prediction data for these models. The dependability of the statistically validated prediction models and their confidence in their predictive powers were improved.

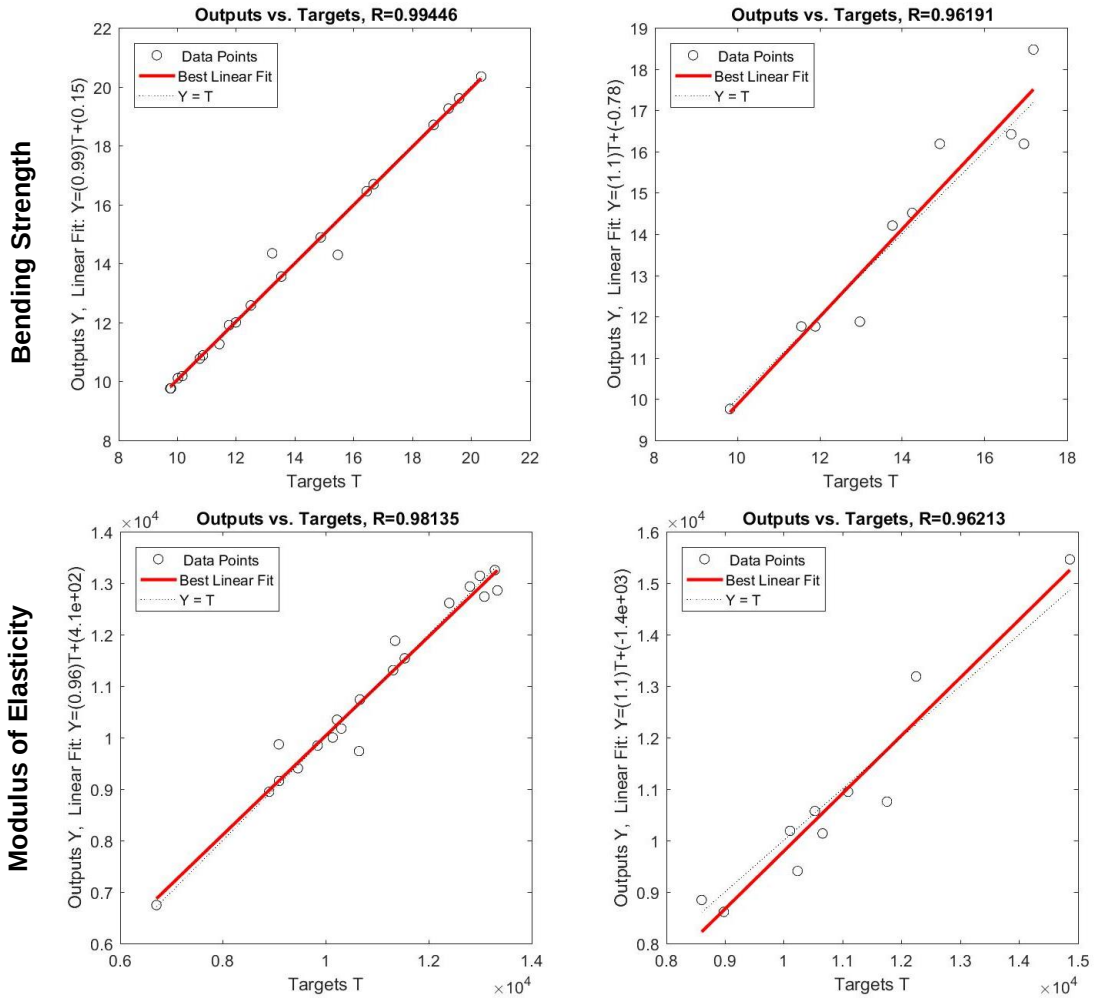

Fig. 7. Regression graphs of bending strength and modulus of elasticity prediction models

Comparisons between the data obtained from experimental studies and the prediction data obtained from ANN models according to the output variables. are presented in Fig. 8.

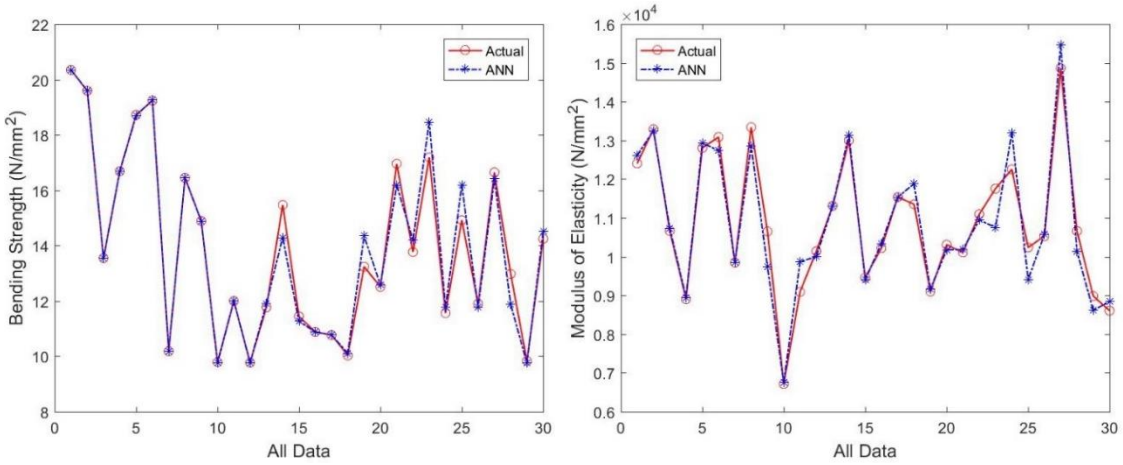

Fig. 8. Comparison of actual data and predicted data

In Fig. 8 it was concluded that the data collected from experimental research closely corresponded to the predicted data generated by the models.

Optimization

Using a high-performance prediction model produced from ANN analysis, it is possible to achieve high accuracy rates in predicting the output data corresponding to the intermediate values of input variables not used in experimental research (Varol *et al*. 2018). The bending strength and modulus of elasticity corresponding to intermediate values of timber strength classes (C14, C18, C20, C27, and D24, D35) not used in experiments were determined as input variables according to TS EN 338 (2016) (C16, C22, C30, and D18, D30, D40). These values were predicted based on the type of wood and the variations of these values according to the timber strength class used in the outer and middle layers of CLT panels. The results are presented in Figs. 9 and 10.

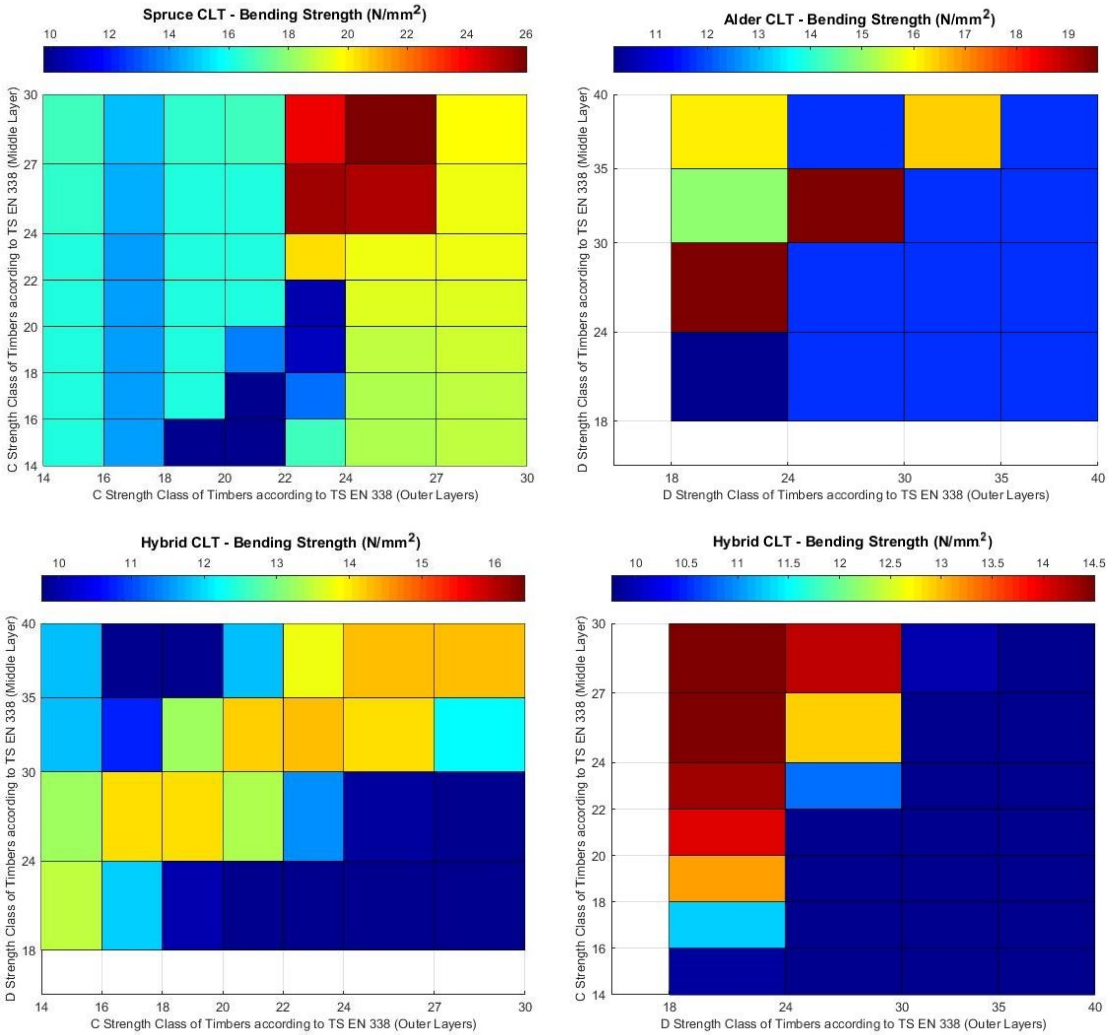

Fig. 9. Change in bending strength values for CLT panels according to timber strength class

When analyzing the fluctuations in the bending strength of CLT panels, it was anticipated that panels constructed from spruce would achieve the highest values of bending strength when the timber strength classes employed in the outer layers are C24

and C27, and for the timbers utilized in the middle layer, the strength classes are C27 and C30. The panels manufactured from alder had the maximum bending strength when the outer layers had a wood strength class of D18 and the center layer had a timber strength class of D24. Additionally, the panels also had high bending strength when the outer layers had a timber strength class of D24 and the inner layers had a timber strength class of D30. The hybrid CLT panels exhibited the greatest bending strength when the spruce was used in the outer layer and alder was used in the intermediate layer, particularly when the panels had a C30-D40 strength class combination. The most optimal results were achieved while using D18 for the outer layers and C24, C27 and C30 for the intermediate layers of hybrid panels which consist of alder in the outer layer and spruce in the center layer.

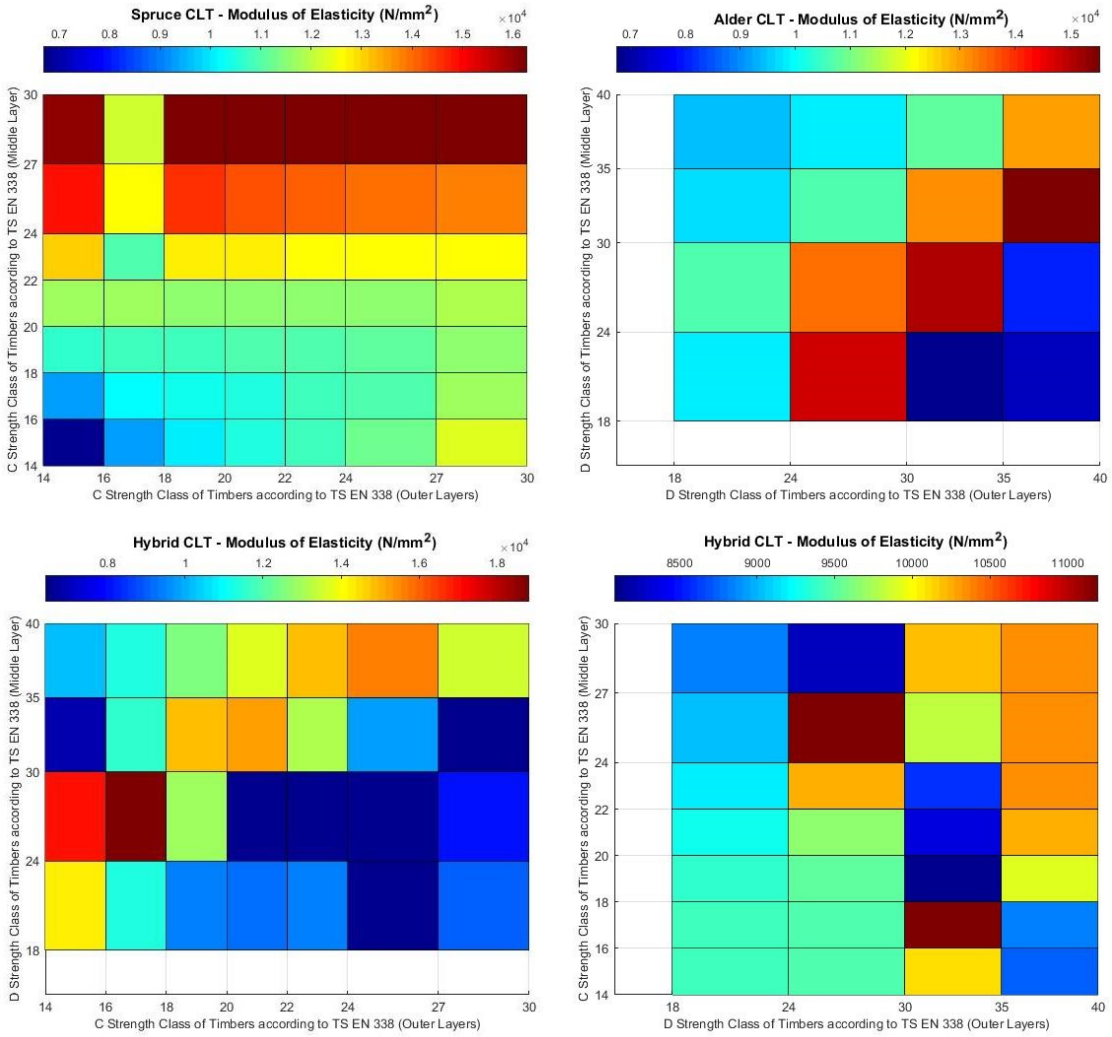

Fig. 10. Change of modulus of elasticity values for CLT panels according to timber strength class

Looking at the differences in the modulus of elasticity of CLT panels, it was predicted that panels made from spruce would have the highest modulus of elasticity values. This would happen when the strength classes of the wood used in the outer layers were between C18 and C30. and between C27 and C30 for the wood used in the middle layer. The panels manufactured from alder exhibited the highest modulus of elasticity values when the outer layers had a timber strength class of D40 and the middle layer had a

timber strength class of D35. Similarly, when the outer layers had a timber strength class of D35 and the middle layer had a timber strength class of D40 the panels likewise showed high modulus of elasticity values. The hybrid CLT panels had the highest modulus of elasticity when they were mixed with a C16-D24 strength class. This was especially true for groups that used spruce in the top layer and alder in the middle layer. The most optimal results were achieved while using D24 and D30 for the outer layers and C16 and C24 for the middle layers of hybrid panels composed of alder and spruce.

The analyses were used to analyze the prediction values of the models developed and based on this, the best timber strength classes and layer combinations were determined according to the type of wood. Table 5 presents the optimal combinations of layers and their related highest values of structural strength.

Table 5. Optimum Timber Strength Class and Layer Combinations for CLT Panels

Structural Strength Properties	Wood Species	Layer Combinations (Outer-Middle-Outer)	Highest Predicted Strength Value (N/mm^2)
Bending Strength	Spruce	C24-C27-C24	26.03
	Alder	D18-D24-D18	19.58
	Hybrid	C30-D40-C30	16.42
	Hybrid	D18-C30-D18	14.51
Modulus of Elasticity	Spruce	C22-C27-C22	16286.57
	Alder	D35-D30-D35	15545.86
	Hybrid	C16-D24-C16	18820.98
	Hybrid	D24-C24-D24	11196.35

Upon analyzing the structural strength data in Table 5, it was noted that CLT panels made from spruce timber had greater bending strength values in comparison to alder and hybrid CLT panels. Nevertheless, it was concluded that hybrid panels provided superior values in relation to the modulus of elasticity. Hybrid panels, consisting of spruce timber in the outer layers and alder timber in the middle layers had a greater modulus of elasticity in comparison to other groups.

Modeling and optimization research is scarce on CLT panels utilizing ANN in the existing literature. Bobadilha *et al.* (2021) employed ANN modeling to analyze color changes in CLT panels exposed to outdoor conditions. Similarly Dong *et al.* (2017) utilized ANN to model the costs and energy consumption associated with CLT. No research has been discovered that particularly examines the mechanical characteristics of CLT panels except for the aforementioned studies. Hence this study offers an innovative perspective and a practical data repository to the existing body of literature.

CONCLUSIONS

1. The best performances of the prediction models for bending strength and modulus of elasticity mean square error (MSE) values were identified at the 500th iteration as 0.0047779 and 0.0066944, respectively.
2. The R-value for the bending strength prediction model was calculated as 0.99446 during the training phase and 0.96191 during the testing phase. For the modulus of

the elasticity prediction model, the R-value was 0.98135 during the training phase and 0.96213 during the testing phase.

3. The MAPE values for bending strength were determined as 1.04% for training data and 3.90% for test data; for modulus of elasticity, the MAPE values were calculated as 1.95% for training data and 4.26% for test data.
4. The RMSE values for bending strength training and test data were calculated as 0.37 and 0.74, respectively; for modulus of elasticity, these values were determined as 333.62 and 585.06, respectively.
5. The optimum timber strength classes and layer combinations were determined for bending strength as C24-C27-C24 for spruce CLT panels. D18-D24-D18 for alder CLT panels, C30-D40-C30 and D18-C30-D18 for hybrid panels.
6. The optimum timber strength classes and layer combinations for modulus of elasticity were determined as C22-C27-C22 for spruce, D35-D30-D35 for alder, C16-D24-C16 and D24-C24-D24 for hybrid CLT panels.

ACKNOWLEDGMENTS

The authors acknowledge the financial support for this study by TUBITAK (The Scientific and Technical Research Council of Turkey) (Project No: 2200012).

REFERENCES CITED

Antanasijević, D. Z., Pocajt, V. V., Povrenović, D. S., Ristić, M. Đ., and Perić-Grujić, A. A. (2013). "PM10 emission forecasting using artificial neural networks and genetic algorithm input variable optimization," *Science of The Total Environment* 443. 511-519. DOI: 10.1016/j.scitotenv.2012.10.110

Bobadilha, G. S., Stokes, C. E., and Verly Lopes, D. J. (2021). "Artificial neural networks modelling based on visual analysis of coated cross laminated timber (CLT) to predict color change during outdoor exposure," *Holzforschung* 75(7), 646-654. DOI: 10.1515/hf-2020-0193

Brandner, R. (2018). "Cross laminated timber (CLT) in compression perpendicular to plane: Testing. properties. Design and recommendations for harmonizing design provisions for structural timber products," *Engineering Structures* 171, 944-960. DOI: 10.1016/j.engstruct.2018.02.076

Demir, A., Demirkir, C., Ozsahin, S., and Aydin, I. (2023). "Artificial neural-network optimization of nail size and spacings of plywood shear wall," *Wood Material Science & Engineering* 18(1), 97-106. DOI: 10.1080/17480272.2021.1992648

Demirkir, C., Özsahin, Ş., Aydin, I., and Colakoglu, G. (2013). "Optimization of some panel manufacturing parameters for the best bonding strength of plywood," *International Journal of Adhesion and Adhesives* 46, 14-20. DOI: 10.1016/j.ijadhadh.2013.05.007

Di Bella, A., and Mitrovic, M. (2020). "Acoustic characteristics of cross-laminated timber systems," *Sustainability* 12(14). article 5612. DOI: 10.3390/su12145612

Dong, Q., Xing, K., and Zhang, H. (2017). "Artificial neural network for assessment of energy consumption and cost for cross laminated timber office building in severe cold regions," *Sustainability* 10(1), article 84. DOI: 10.3390/su10010084

Dong, W., Wang, Z., Chen, G., Wang, Y., Huang, Q., and Gong, M. (2023). "Bonding performance of cross-laminated timber-bamboo composites," *Journal of Building Engineering* 63, article ID 105526. DOI: 10.1016/j.jobe.2022.105526

Follesa, M., and Fragiacomo, M. (2018). "Force-based seismic design of mixed CLT/light-frame buildings," *Engineering Structures* 168, 628-642. DOI: 10.1016/j.engstruct.2018.04.091

Guo, H., Liu, Y., Chang, W. S., Shao, Y., and Sun, C. (2017). "Energy saving and carbon reduction in the operation stage of cross laminated timber residential buildings in China," *Sustainability* 9(2), article 292. DOI: 10.3390/su9020292

Hadigheh, S. A., and Dias-da-Costa, D. (2020). "Shear strength of cross laminated timber-concrete connections reinforced with carbon fibre polymer composites," in: *ACMSM25*, Springer, Singapore, pp. 179-185.

Hassanieh, A., Valipour, H. R., and Bradford, M. A. (2017). "Experimental and numerical investigation of short-term behaviour of CLT-steel composite beams," *Engineering Structures* 144, 43-57. DOI: 10.1016/j.engstruct.2017.04.052

Hematabadi, H., Madhoushi, M., Khazaeyan, A., Ebrahimi, G., Hindman, D., and Loferski, J. (2020). "Bending and shear properties of cross-laminated timber panels made of poplar (*Populus alba*)," *Construction and Building Materials* 265, article ID 120326. DOI: 10.1016/j.conbuildmat.2020.120326

Hindman, D. P., and Golden, M. V. (2020). "Acoustical properties of southern pine cross-laminated timber panels," *Journal of Architectural Engineering* 26(2), article ID 05020004. DOI: 10.1061/(ASCE)AE.1943-5568.0000407

Karacabeyli, E., and Gagnon, S. (2019). *Canadian CLT Handbook*, FPInnovations, Quebec, Canada.

Kippel, M., Leyder, C., Frangi, A., Fontana, M., Lam, and Ceccotti. F. (2014). "Fire tests on loaded cross-laminated timber wall and floor elements," *Fire Safety Science* 11, 626-639. DOI: 10.3081/IAFSS.FSS.11-626

Küçükönder, H., Boyaci, S., and Akyüz, A. (2016). "A modeling study with an artificial neural network: Developing estimation models for the tomato plant leaf area," *Turkish Journal of Agriculture and Forestry* 40(2), 203-212. DOI: 10.3906/tar-1408-28

Liao, Y., Tu, D., Zhou, J., Zhou, H., Yun, H., Gu, J., and Hu, C. (2017). "Feasibility of manufacturing cross-laminated timber using fast-grown small diameter eucalyptus lumbers," *Construction and Building Materials* 132, 508-515. DOI: 10.1016/j.conbuildmat.2016.12.027

Lie, X., Subhani, M., Ashraf, M., Kafle, B., and Kremer, P. (2020). "A current-state-of-the-art on design rules vs test resistance of cross laminated timber members subjected to transverse loading," in: *CIGOS 2019. Innovation for Sustainable Infrastructure*, Springer, Singapore, pp. 185-190.

Luengo, E., Hermoso, E., Cabrero, J. C., and Arriaga, F. (2017). "Bonding strength test method assessment for cross-laminated timber derived stressed-skin panels (CLT SSP)," *Materials and Structures* 50(4), article 204. DOI: 10.1617/s11527-017-1069-8

Marko, G., Bejó, L., and Takats, P. (2016). "Cross-laminated timber made of Hungarian raw materials," *IOP Conference Series: Materials Science and Engineering* 123(1), article ID 012059. DOI: 10.1088/1757-899X/123/1/012059

O'Dowd, B., Cunningham, L., and Nedwell, P. (2016). "Briefing experimental and theoretical bending stiffness of cross-laminated timber panels," *Proceedings of the Institution of Civil Engineers - Construction Materials* 169(6), 277-281. DOI: 10.1680/jcoma.15.00063

Ozturk, H., Demir, A., and Demirkir, C. (2022). "Optimization of pressing parameters for the best mechanical properties of wood veneer/polystyrene composite plywood using artificial neural network," *European Journal of Wood and Wood Products* 80(4), 907-922. DOI: 10.1617/s11527-017-1069-8

Özşahin, Ş. (2012). "The use of an artificial neural network for modelling the moisture absorption and thickness swelling of oriented strand board," *BioResources* 7(1), 1053-1067. DOI: 10.15376/biores.7.1.1053-1067

Reynolds, T., Foster, R., Bregulla, J., Chang, W. S., Harris, R., and Ramage, M. (2017). "Lateral-load resistance of cross-laminated timber shear walls," *Journal of Structural Engineering* 143(12), 06017006-1-06017006-6. DOI: 10.1061/(ASCE)ST.1943-541X.0001912

Satir, E. (2023). *Mechanical Properties of Hybrid Softwood and Hardwood Cross-Laminated Timbers*, *Master of Science Thesis*, Virginia Tech University, Blacksburg. VA, USA. https://vtechworks.lib.vt.edu/bitstreams/cffcd4af-ee23-4ee3-89de-0c78ee8449ea/download

Shi, X., Yue, K., Jiao, X., Zhang, Z., and Li, Z. (2023). "Experimental investigation into lateral performance of cross-laminated timber shear walls made from fast-growing poplar wood," *Wood Material Science & Engineering* 18(4), 1212-1227. DOI: 10.1080/17480272.2022.2121659

Soriano, F. M., Pericot, N. G., and Sierra, E. M. (2016). "Comparative analysis of the reinforcement of a traditional wood floor in collective housing. In depth development with cross laminated timber and concrete," *Case Studies in Construction Materials* 4, 125-145. DOI: 10.1016/j.cscm.2016.03.004

Srivaro, S., Tomad, J., Shi, J., and Cai, J. (2020). "Characterization of coconut (*Cocos nucifera*) trunk's properties and evaluation of its suitability to be used as raw material for cross laminated timber production," *Construction and Building Materials* 254, article ID 119291. DOI: 10.1016/j.conbuildmat.2020.119291

Taşpınar, F., and Bozkurt, Z. (2014). "Application of artificial neural networks and regression models in the prediction of daily maximum PM10 concentration in Düzce, Turkey," *Fresenius Environmental Bulletin* 23(10), 2450-2459.

TS EN 408 (2014). "Timber structures – Structural timber and glued laminated timber – Determination of some physical and mechanical properties," Turkish Standards Institution, Ankara, Turkey.

TS 1265 (2012). "Sawn timber (Coniferous) – For building construction," Turkish Standards Institution, Ankara, Turkey.

TS EN 14081 (2019). "Timber structures – Strength graded structural timber with rectangular cross section – Part 1: General requirements," Turkish Standards Institution, Ankara, Turkey.

TS EN 338 (2016). "Structural timber – Strength classes," Turkish Standards Institution, Ankara, Turkey.

Turesson, J., Berg, S., and Ekevad, M. (2019). "Impact of board width on in-plane shear stiffness of cross-laminated timber," *Engineering Structures* 196, article ID 109249. DOI: 10.1016/j.engstruct.2019.05.090

Varol, T., Canakci, A., and Ozsahin, S. (2018). "Prediction of effect of reinforcement content. Flake size and flake time on the density and hardness of flake AA2024-SiC nanocomposites using neural networks," *Journal of Alloys and Compounds* 739, 1005-1014. DOI: 10.1016/j.jallcom.2017.12.256

Wieruszewski, M., and Mazela, B. (2017). "Cross laminated timber (CLT) as an alternative form of construction wood," *Drvna Industrija* 68(4), 359-367. DOI: 10.5552/drind.2017.1728

Yadav, V., and Nath, S. (2017). "Forecasting of PM 10 using autoregressive models and exponential smoothing technique," *Asian Journal of Water, Environment and Pollution* 14(4), 109-113. DOI: 10.3233/AJW-170041

Article submitted: February 8, 2024; Peer review completed: May 27, 2024; Revised version received: May 30, 2024; Accepted: June 1, 2024; Published: June 4, 2024.
DOI: 10.15376/biores.19.3.4899-4917